EPJ Web of Conferences **93**, 01039 (2015)
DOI: 10.1051/epjconf/20159301039

Observation of low-lying resonances in the quasicontinuum of ^{195,196}Pt and enhanced astrophysical reaction rates

F. Giacoppo[1,a], F. L. Bello Garrote[1], T. K. Eriksen[1], A. Görgen[1], M. Guttormsen[1], T. W. Hagen[1], A. C. Larsen[1], B. V. Kheswa[1,2], M. Klintefjord[1], P. E. Koehler[3], L. G. Moretto[4], H. T. Nyhus[1], T. Renstrøm[1], E. Sahin[1], S. Siem[1], and T. G. Tornyi[1,5]

[1] *Department of Physics, University of Oslo, N-0316 Oslo, Norway*
[2] *Department of Physics, University of Stellenbosch, 7602 Stellenbosch, South Africa*
[3] *Air Force Technical Applications Center, Patrick Air Force Base, Florida, USA*
[4] *Lawrence Berkeley National Laboratory, 1 Cyclotron Road, Berkeley, California 94720, USA*
[5] *Institute of Nuclear Research of the Hungarian Academy of Sciences, H-4001 Debrecen, Hungary*

Abstract. An excess of strength on the low-energy tail of the giant dipole resonance recently has been observed in the γ-decay from the quasicontinuum of ^{195,196}Pt. The nature of this phenomenon is not yet fully investigated. If this feature is present also in the γ-ray strength of the neutron-rich isotopes, it can affect the neutron-capture reactions involved in the formation of heavy-elements in stellar nucleosynthesis. The experimental level density and γ-ray strength function of ^{195,196}Pt are presented together with preliminary calculations of the corresponding neutron-capture cross sections.

1 Introduction

In the last decades, enhancements in the γ transition probability at energies below the giant dipole resonance (GDR) region have been observed in several nuclei [1]. Interest in such resonance-like phenomenon is driven by the understanding of the underlying nuclear structure. For medium-mass and heavy nuclei, a collective interpretation cannot fully describe the experimental data and more complex configurations, including coupling of single-particle excitations, have to be taken into account.

Moreover, the presence of resonances in the vicinity of the neutron threshold may have profound implications for the heavy-element nucleosynthesis [2]. In particular the element Pt is predominantly produced in rapid neutron-capture (r-) processes, although the astrophysical scenario where the (n,γ) reaction chains take place is currently under debate [3]. The Pt isotopes are located at the $A \sim 195$ r-process peak in the solar-system element abundance. Therefore the availability of direct data in this region is essential to obtain with reasonable accuracy the relevant (n,γ) reaction rates for the most neutron-rich isotopes through statistical model calculations [4].

The properties of stable ^{195,196}Pt for excitation energies in the quasicontinuum have been recently investigated at the Oslo Cyclotron Laboratory (OCL). The nuclear level density and the γ-ray strength function, which is the average electromagnetic response of the nucleus, were determined in particle-γ coincidence measurements, using the Oslo method [5]. These are the key input parameters used in the Hauser-Feshbach formalism to determine neutron-capture cross sections. In this work, special attention is given to the enhancements observed in the γ-ray strength functions and their impact in the calculated neutron-capture cross section and astrophysical reaction rates.

These results are part of a more extensive investigation of the electromagnetic decay properties of nuclei in the $A = 195$ region of the valley of stability. For all these nuclei the γ emission from the quasicontinuum is characterized by resonance structures close to the neutron separation threshold.

2 Experimental setup and data analysis

The ^{195}Pt(p,p') and ^{195}Pt(d,p) reactions were studied using a self-supporting target with a thickness of $\sim$1.5 mg/cm^2. The targets were irradiated with a proton beam at 16.5 MeV and a deuteron beam at 11.3 MeV, delivered by the MC-35 Scanditronix cyclotron at OCL. Particle-γ coincidence events were measured by the Silicon Ring (SiRi) particle detector system [6] and the CACTUS multi-detector system [7]. SiRi is an annular array of eight trapezoidal silicon $\Delta E - E$ telescopes, mounted at 5 cm distance from the target. It covers scattering angles between 126^o and 140^o with respect to the beam direction, with a resolution of $\Delta\theta = 2^o$. Each telescope consists of a 8-fold segmented thin detector (130 μm) and a thick single Si crystal (1550 μm). CACTUS is a spherical array of 26 collimated 5"×5" NaI(Tl) γ-ray detectors surrounding the

[a] e-mail: francesca.giacoppo@fys.uio.no

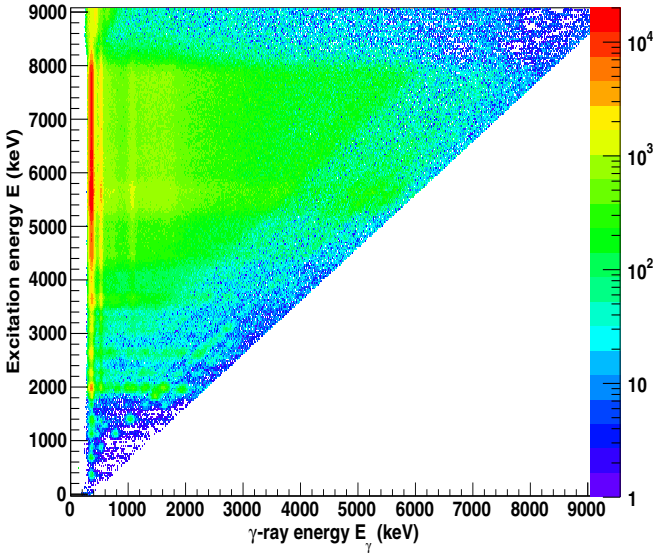

Figure 1. Particle-γ coincidence matrix for ^{195}Pt$(d, p\gamma)^{196}$Pt, unfolded with the NaI response functions. The γ emission drops above S_n = 7922 keV where the $(d, pn\gamma)$ channel is open.

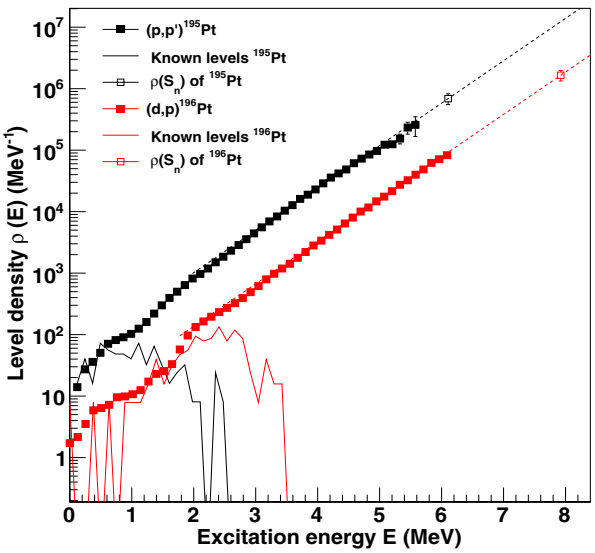

Figure 2. Nuclear level density of ^{195}Pt (black filled squares) and ^{196}Pt (red filled squares) normalized to the density of discrete levels at low energy (black and red lines, respectively) and to $\rho(S_n)$ at high energy (black and red open squares, respectively). Both experimental distributions have a trend compatible with the constant temperature extrapolation (black and red dotted lines) with a common temperature T = 0.63 MeV [20].

target point. Its total detection efficiency is 14.1(1)% at E_γ= 1332 keV.

By coupling the energy deposited into the ΔE detector with the E detector, the different types of charged particles are uniquely identified. Hence, the excitation energy of the residual nucleus is reconstructed, with a resolution of 100-150 keV, from the reaction kinematics and Q-value, the energy and angle of the emitted particle. The spectrum of emitted γ-rays, tagged in excitation energy of the residual nucleus, is corrected for the detector response function through an unfolding procedure, as shown in Fig. 1 for ^{196}Pt [8]. At this stage of the analysis, an iterative subtraction technique is applied to filter the distribution of primary γ transitions from the following generations of γ-rays belonging to the cascades originating from states at a given excitation energy [9]. The matrix of first-generation γ-rays $P(E, E_\gamma)$ expresses the probability of a γ-ray with energy E_γ decaying from a specific excitation energy E.

In the regime of statistical decay processes, the reaction occurs through the formation of a compound nucleus and the relative decay probability to a certain final state is independent of the way the compound system is formed [10]. Therefore, P can be factorized in the product of the level density at the final excitation energy $\rho(E - E_\gamma)$ and the γ transition probability between the initial and the final states:

$$P(E, E_\gamma) \propto \rho(E - E_\gamma)\mathcal{T}(E_\gamma) \qquad (1)$$

where the transmission coefficient $\mathcal{T}(E_\gamma)$ and the γ-ray strength function $f(E_\gamma) = \mathcal{T}(E_\gamma)/2\pi E_\gamma^3$ are proportional and approximately independent of the excitation energy [11, 12]. Furthermore, only dipole transitions are taken into account, being the dominant decay mode from states in the quasicontinuum [13].

Eq. (1) allows the disentanglement of the level density and the γ-ray strength function through a simultaneous least-square fit of $P(E, E_\gamma)$. Since no initial assumptions are made on ρ and f, only their functional form can be extracted. In order to obtain the absolute curves, two scale parameters and a common slope coefficient need to be determined from independent experimental data. To estimate the common slope, the level density is normalized to two anchor points: the density of low-energy discrete levels taken from literature [14] and the level density at the neutron separation energy $\rho(S_n)$. The latter point can be calculated with a simple expression when experimental values of the s-wave neutron resonance spacing D_0 are available [15]. We assume that the number of positive and negative parity levels at S_n is equal, which is a good approximation for heavy not-magic nuclei. To properly estimate $\rho(S_n)$ with this procedure, the spin distribution should be taken into account. Since it is impossible to measure experimentally this quantity when the number of levels is too high, we rely on an empirical formula that describes a gaussian-like spin distribution with a width parameter σ, the spin cutoff [16–18]:

$$g(J, \sigma) \simeq \frac{2J+1}{2\sigma^2} e^{-\frac{J(J+1)}{2\sigma^2}}. \qquad (2)$$

More details on the normalization procedure can be found in Refs. [5, 19]. The normalization of the level density of the Pt isotopes is shown in Fig. 2 and has been presented in Ref. [20].

Finally, the absolute γ-ray strength function is determined when the radiative width calculated with the experimental ρ and $\mathcal{T}$ is scaled to the average total radiative width $\langle \Gamma_{\gamma 0} \rangle$ at S_n from s-wave neutron resonance de-

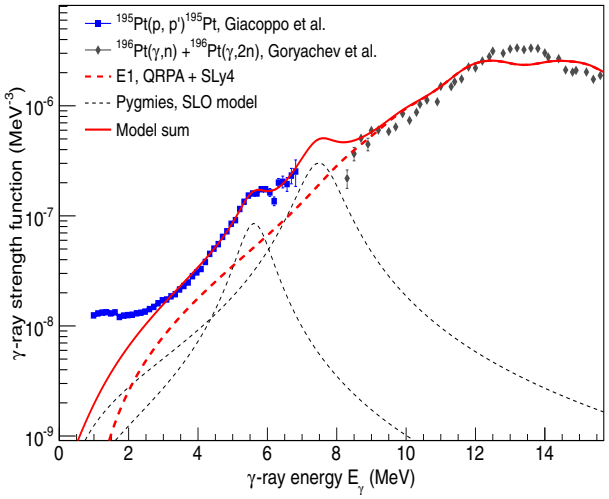

Figure 3. Preliminary γ-ray strength function of ^{195}Pt from the present work (blue filled squares) together with photonuclear data (black filled diamonds) [21]. The QRPA model (dotted red line) is applied to fit the E1 strength in correspondence of the GDR and its tail [22]. The excess of strength below the neutron separation energy is fitted with two Standard Lorentzian functions. More details are given in the text.

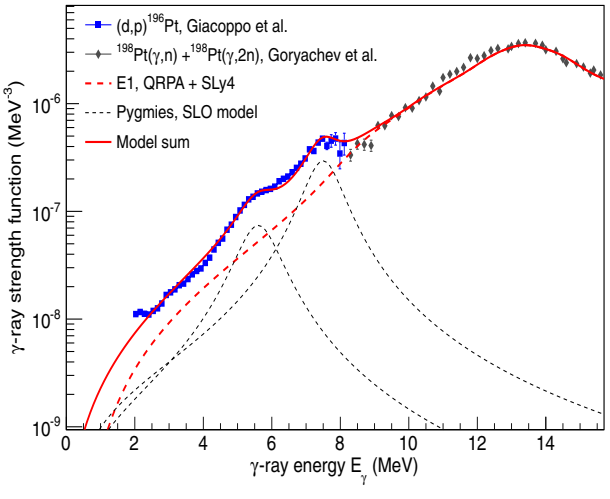

Figure 4. Preliminary γ-ray strength function of ^{196}Pt (blue filled squares) compared with data from Ref. [21] and model predictions. A double resonance is observed below the neutron separation energy with energy centroids at about 5.64 and 7.52 MeV. See Fig. 3 and the text for more details.

cay [15]:

$$\left\langle \Gamma_\gamma(S_n, J^\pi) \right\rangle = \frac{B}{4\pi\rho(S_n, J_i^\pi)} \int_0^{S_n} dE_\gamma \mathcal{T}(E_\gamma) \times \\ \times \rho(S_n - E_\gamma) \sum_{J_f} g(S_n - E_\gamma, J_f) \qquad (3)$$

where B is the normalization parameter, $J_i^\pi = I_i^\pi \pm 1/2$ the initial spin and parity and depends on the spin and parity of the target nucleus in the corresponding (n,γ) reaction. The integration includes all the final states with spin J_f assuming the spin and parity distribution as described above.

3 Preliminary results

The total γ-ray strength functions of ^{195,196}Pt are presented in Fig. 3 and 4. An uncertainty of $\approx$ 20% has to be taken into account, due to the normalization procedure. In the same Figures, a comparison with photonuclear data from Ref. [21] is shown. The (γ, n) and $(\gamma, 2n)$ cross-sections $\sigma(E_\gamma)$ are converted into γ-strengths $f(E_\gamma)$ through the relation:

$$f(E_\gamma) = \frac{1}{3(\pi\hbar c)^2} \frac{\sigma(E_\gamma)}{E_\gamma}. \qquad (4)$$

The experimental data are also compared with model predictions. Microscopic calculations of the electric dipole strength based on the quasiparticle random-phase approximation (QRPA) with the SLy4 Skyrme force [22] are here included in order to reproduce the GDR and its tail at low energies.

For both Pt isotopes an excess of strength is observed between 4.0 and 7.0 MeV that has been fitted with a Standard Lorentzian (SLO) function with an energy centroid of E_γ=5.64(3) MeV and a width of Γ=1.3(2) MeV. This resonance exhausts about 0.34% of the Thomas-Reiche-Kuhn (TRK) sum rule. For ^{196}Pt, states at higher excitation energy has been populated during the reaction: one can observe a second enhancement centered at about 7.5 MeV, just below the neutron threshold where the Oslo data are coupled to the photoneutron γ-strength. This work confirms the presence of a double-humped structure in the electromagnetic response of the quasicontinuum in ^{196}Pt, which corresponds to $\approx$ 0.34 + 1.62 $\approx$ 1.96% of the total integrated strength. In a recent (γ,γ') experiment, the ground-state photo-absorption cross section of ^{196}Pt displays two resonances in the same energy region as in the present work [23]. For ^{195}Pt, the data set ranges from E_γ = 1.0 MeV to 6.8 MeV and, although a new increase of the γ-strength is observed above the first peak, it is not possible to establish whether the resonance structure at 7.5 MeV is present also for the odd-even Pt isotope (see model fit in Fig. 3).

The present experimental technique does not allow to disentangle the electric and magnetic components of the γ-strength. Complementary experiments are needed to fully characterize the nature of the observed structures that cover the energy window where both the magnetic dipole spin-flip and the E1 pygmy dipole resonance are expected. From average neutron resonance data there is evidence of a concentration of E1 transitions in the proximity of the neutron separation threshold [24]. From systematics and available experimental data, one estimates that less then 10% of the strength in this energy region should be due to magnetic transitions [25, 30].

It is interesting to mention that an excess of strength is observed also at energies below E_γ = 2 MeV in ^{195}Pt. It is compatible with a weak and broad distribution in

the energy domain where the M1 scissor resonance is expected [30] and has been observed for the even-even adjacent isotopes, ^{194}Pt and ^{196}Pt [31, 32].

4 Neutron capture cross sections

To investigate the impact of the pygmy resonances on astrophysical (n,γ) reaction rates, we have performed statistical calculations of the radiative neutron-capture reactions ^{194}Pt$(n,\gamma)^{195}$P and ^{195}Pt$(n,\gamma)^{196}$Pt using the reaction code TALYS [27]. We have included information of the experimentally extracted level densities [20] which are well reproduced, above the pair-breaking region ($E > 2\Delta \approx 2$ MeV), by the constant temperature model [17] using the parameterization from [18]. A common temperature of $T = 0.63$ MeV has been obtained for both nuclei from a fit to the experimental data. At the same time an energy shift of $E_0 = -2.07$ MeV and -0.81 MeV has been determined for ^{195,196}Pt, respectively. Another ingredient for the cross-section calculations are the γ-strength functions presented previously in this work. For both Pt isotopes we assume a double-humped resonance where the lower-energy component at $E_\gamma \approx 5.6$ MeV is of M1 type while the one at $E_\gamma \approx 7.5$ MeV is of E1 type. We have tested that inverting the electromagnetic characters will give a relative difference of maximum 6% in the calculated cross sections. No further normalization is applied to the γ strength function ($G_{norm} = 1$), in order to test the unaltered contribution of the experimental data in the nuclear reaction calculations. With the experimental inputs, the total radiative width is well reproduced within 10% from the reference value of Ref. [15]. For the neutron optical-model potential we adopt the suggested phenomenological parameterization of [28] that is implemented in TALYS. We apply an adjustment of the parameters a_V and a_D according to the findings of Ref. [15]. Fig. 5 shows the resulting calculated cross sections compared with direct (n,γ) measurements from Refs. [15, 29]. Especially for $(n,\gamma)^{196}$Pt, there is an excellent agreement between the calculations and the data.

Clearly, the enhanced strengths impact the (n,γ) cross sections, giving, for instance, an increase of $\approx$ 166% for 1 MeV incoming neutrons for the production of both ^{195,196}Pt. At the same time, the astrophysical (n,γ) reaction rates are increased by a factor of about two when the observed resonances are included.

As shown in Ref. [2], such resonance structures in the vicinity of the neutron threshold may have profound implications for the heavy-element nucleosynthesis. Platinum isotopes are of special importance, since they are located at the $A \approx 195$ r-process peak. Therefore the experimental confirmation of such structures in this region is essential to obtain a reasonable accuracy of the relevant (n,γ) reaction rates.

5 Summary and outlook

An excess of strength has been observed on the tail of the GDR of ^{195,196}Pt, due to γ-decay from the quasicontinuum. In both isotopes, the extra strength is concentrated around

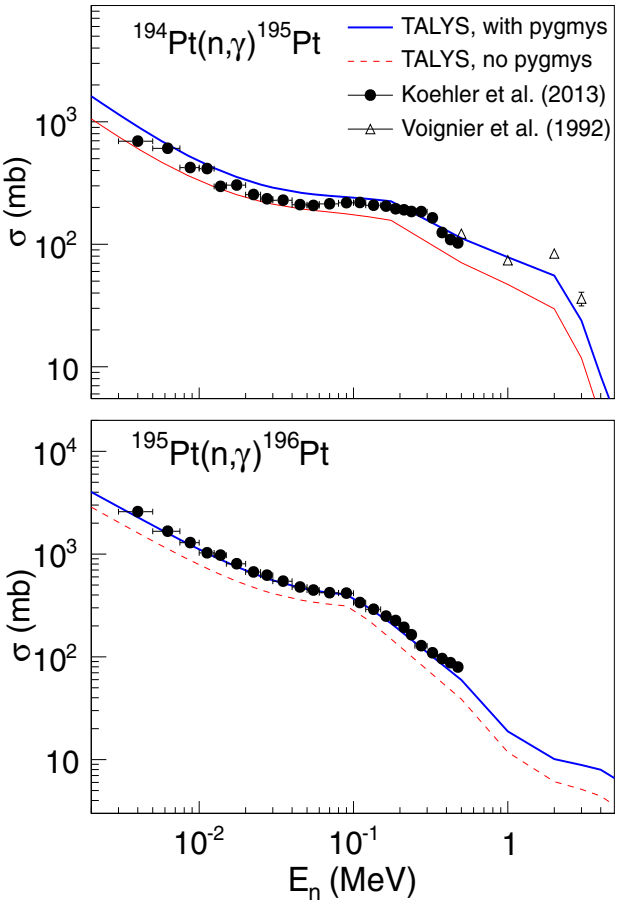

Figure 5. Neutron-capture cross sections for (top) ^{194}Pt$(n,\gamma)^{195}$Pt and (bottom) ^{195}Pt$(n,\gamma)^{196}$Pt. Calculations with the TALYS code has been performed with (solid blue line) and without (solid red line) the low-energy resonance structures in the input γ-ray strength functions. The calculations including the strength enhancement are in good agreement with (n,γ) data from Refs. [15, 29].

$\approx$ 5.6 MeV. In ^{196}Pt a second peak is present just below the neutron separation threshold. This double-humped enhancement is non-trivial and further experimental studies are needed to identify the nuclear structure properties that are responsible for the splitting of the strength.

The element platinum (Z=78) is of special interest from an astrophysical point of view, since it is produced predominantly in r-process nucleosynthesis. This nuclear mass region defines one of the three major r-process peaks identified in the solar system r-process abundance pattern. Depending on the physical conditions at the r-process site, nuclear properties such as resonances in the γ-strength could significantly change the neutron-capture reaction rates, with possible implications for the final calculated abundances.

Experimental data of very neutron-rich nuclei in the Pt mass region are requested in order to investigate and characterize these resonances when they are present in the electromagnetic response. It is expected to observe more pro-

nounced peaks moving from the stability towards the neutron drip line. However, the quasicontinuum of neutron-rich nuclei in this mass region is so far very difficult to access experimentally. Hence, one has to rely on model calculations for the dipole strength distribution of these nuclei. This demands for a detailed understanding of the nature of the low-lying E1 strength in microscopic models. To ensure high predictive power for very neutron-rich systems, the latter should be tested for stable or close-to-stability nuclear systems. In this context, additional experiments are planned in order to study the evolution of the resonance structures in heavy nuclei below the double-magic ^{208}Pb.

References

[1] D. Savran *et al.*, Prog. Part. Nucl. Phys. **70**, 210 (2013)

[2] S. Goriely, Phys. Lett. B **436**, 10 (1998)

[3] M. Arnould *et al.*, Physics Reports **450**, 97 (2007)

[4] W. Hauser and H. Feshbach, Phys. Rev. **87**, 366 (1952)

[5] A. Schiller *et al.*, Nucl. Instrum. Methods Phys. A **447**, 498 (2000)

[6] M. Guttormsen *et al.*, Nucl. Instrum. Methods Phys. Res. A **648**, 168 (2011)

[7] M. Guttormsen *et al.*, Phys. Scr. **T32**, 54 (1990)

[8] M. Guttormsen *et al.*, Nucl. Instrum. Methods Phys. Res. A **374**, 371 (1996)

[9] M. Guttormsen *et al.*, Nucl. Instrum. Methods Phys. Res., Sect. A **255**, 518 (1987)

[10] A. Bohr and B. Mottelson, *Nuclear Structure* Vol. I, Benjamin, New York (1969)

[11] D. M. Brink, PhD thesis, Oxford University (1995)

[12] P. Axel, Phys. Rev. **126**, 671 (1962)

[13] J. Kopechy and M. Uhl, Phys. Rev. C **41**, 1941 (1990)

[14] National Nuclear Data Center On-Line Data Service for the ENSDF database, URL: http://www.nndc.bnl.gov/ensdf/

[15] P. E. Koehler, K. H. Guber, Phys. Rev. C **88**, 035802 (2013)

[16] T. Ericson, Advances in Physics **9**, 425 (1960)

[17] A. Gilbert and A. G. W. Cameron, Can. Jour. Phys. **43**, 1446 (1965)

[18] T. von Egidy and D. Bucurescu, Phys. Rev. C **80**, 054310 (2009)

[19] A. C. Larsen *et al.*, Phys. Rev. C **83**, 034315 (2011)

[20] F. Giacoppo *et al.*, Phys. Rev. C **90**, 054330 (2014)

[21] A. M. Goryachev and G. N. Zalesnyy, Sov. J. Nucl. Phys. **27**, 779 (1978) [Yad. Fiz. **27**, 1479 (1978)]

[22] S. Goriely and E. Khan, Nucl. Phys. A **706**, 217 (2002)

[23] R. Massarczyk *et al.*, Phys. Rev. C **87**, 044306 (2013)

[24] S. F. Mughabghab and C. L. Dunford, Phys. Lett. B **487**, 155 (2000)

[25] T. Belgya *et al.*, *Handbook for calculations of nuclear reaction data, RIPL-2*. IAEA-TECDOC-1506 (IAEA, Vienna, 2006). URL: http://www-nds.iaea.org/RIPL-2/; R. Capote *et al.*, *Reference Input Parameter Library RIPL-3*, Nucl. Data Sheets 110, 3107 (2009), URL: http://www-nds.iaea.org/RIPL-3/

[30] A. Richter, Prog. Part. Nucl. Phys. **34**, 261 (1995)

[27] A. J. Koning *et al.*, TALYS-1.4, in *Nuclear Data for Science and Technology*, EDP Sciences; Editors: O. Bersillon, F. Gunsing, E. Bauge, R. Jacqmin, and S. Leray, EDP Sciences, 211 (2008), URL: http://www.talys.eu/

[28] A. J. Koning and J. P. Delaroche, Nucl. Phys. A **713**, 231 (2003)

[29] J. Voignier *et al.*, Nuclear Science and Engineering **112**, 87 (1992)

[30] A. Richter, Prog. Part. Nucl. Phys. **34**, 261 (1995)

[31] A. Linnemann *et al.*, Phys. Lett. B **544**, 15 (2003)

[32] P. von Brentano *et al.*, Phys. Rev. Lett. **76**, 2029 (1996)